JOURNAL OF CHROMATOGRAPHY A

INCLUDING ELECTROPHORESIS AND OTHER SEPARATION METHODS

ELSEVIER

Amsterdam – Lausanne – New York – Oxford – Shannon – Tokyo

0021-9673/95/$09.50

ELSEVIER

Journal of Chromatography A, 718 (1995) 1–8

JOURNAL OF CHROMATOGRAPHY A

Liquid chromatographic process identification using pulse testing techniques
Applications to column standardization and scale-up☆

Joseph C. Dalton[a], Shalabh Gupta[a], Mark D. Bruley[b], Kyung A. Kang[a], Duane F. Bruley[a]*

[a] *Department of Chemical and Biochemical Engineering, University of Maryland Baltimore County (UMBC), Baltimore, MD 21228, USA*

[b] *Synthesizer Inc., Columbia, MD 21045, USA*

First received 29 December 1994; revised manuscript received 6 June 1995; accepted 12 June 1995

Abstract

Transfer functions have been obtained from frequency response analysis via liquid chromatographic pulse testing and Bode diagrams. The system order of the transfer function, within the range tested, is dependent on the anion-exchange gel characteristics, and not on packing height or pulse sample size. It is also observed that as the activity of the anion-exchange gel decreased, the system order of the transfer function decreased. This unique identification strategy could have great potential for the design of automatic control systems, and the standardization of chromatographic systems for Food and Drug Administration process validation. The ultimate goal, however, would be to verify phenomenological models to facilitate process scale-up for the commercialization of bioproducts.

1. Introduction

Over the past 30 years, chromatography has developed into an indispensable technique for protein purification. With such widespread use, process identification, scale-up, and validation are primary focus issues. To date, most scale-up and validation techniques are still accomplished via "seat of the pants" modifications relying on the expertise and experience of the operators. In this work, a preliminary study has been made to apply the principles of frequency response analysis [1] to develop a transfer function for liquid chromatographic system identification.

Pulse testing, to obtain frequency response data, has long been accepted as a practical technique for process identification [2–5]. Chromatography has benefited from pulse testing for parameter evaluation [6–8], although the underlying assumptions for its use in physico-chemical parameter evaluation have not been the subject of a detailed investigation. Until now, transfer functions have not been used to model chromatographic systems. The advantage of using

* Corresponding author. Address for correspondence: Bioengineering Program, UMBC, ECS 202-A, 5401 Wilkens Avenue, Baltimore, MD 21228, USA.

☆ Presented at *the Workshop on Chromatography, Electrokinetics, and Separations in Porous Media, Gaithersburg, MD, 4–5 August 1994.*

0021-9673/95/$09.50
SSDI 0021-9673(95)00664-8

this technique is that the transfer function must empirically match both the phase angle and the magnitude ratio simultaneously, thus providing a system check that does not exist within the time domain. Therefore, by relating physical parameters to variables in the frequency domain of the transfer function [3–5], a potentially powerful tool for chromatographic system identification is employed.

2. Theory

The application of pulse testing to chromatography treats the system as a black box. Once the system is at equilibrium, a disturbance is added, and system response is recorded until re-equilibration.

The disturbance is the fundamental requirement for any process identification technique. While sinusoidal inputs are the classical disturbance, these are difficult to generate for processes like chromatography. The use of a single input pulse as the disturbance allows for a frequency response over a range of frequencies. With an appropriately sharp pulse, approximating a Dirac delta function, a wide range of response frequencies can be achieved. The pulse is small enough not to overload the column, thereby avoiding non-linear behavior. Non-linear operation using overloaded gradients have been under investigation by Guiochon and co-workers [9].

The system response is recorded as a function of time and then, using Fourier transforms [4,10], the data is reduced to the frequency domain,

$$F(\omega) = \int_{\infty}^{-\infty} f(t)\, e^{-j\omega t}\, dt \tag{1}$$

where $f(t)$ is the time domain pulse data, $F(\omega)$ is the pulse data in the Fourier domain, t is the time, j is the imaginary number, and ω is the frequency. In theory, the integral would be over an interval from positive to negative infinity. For pulses, however, the interval begins and ends at zero. Thus, the integration time limits for both the input and output functions are zero. The system response in the Fourier domain is defined as the transfer function $G(\omega)$. A transfer function is a method of translating the dynamic behavior of a system's input and output signals into the Laplace or Fourier domain. Once in the Laplace or Fourier domain, mathematical calculations for exponential relationships, and interpretations on relationships become simpler. When the forcing frequency (ω) is substituted for s (Laplace variable), a transfer function in the frequency domain results:

$$G(\omega) = \frac{Y(\omega)}{X(\omega)} = \frac{\int_{0}^{T_y} y(t)\, e^{-j\omega t}\, dt}{\int_{0}^{T_x} x(t)\, e^{-j\omega t}\, dt} \tag{2}$$

where T_x and T_y are the pulse input and output times, respectively.

When reducing experimental pulse data, the normalized input frequency content (NFC) is useful for discerning when the transformed data has become too noisy for use. The NFC is defined as:

$$NFC = \frac{\left| \int_{0}^{T_x} x(t)\, e^{-j\omega t}\, dt \right|}{\left| \int_{0}^{T_x} x(t)\, dt \right|} \tag{3}$$

NFC can vary between values of 0 and 1, and decreases with increasing forcing frequency. As a rule-of-thumb, when the NFC falls below 0.3, results are deemed unstable. The sharper the input pulse, the greater the range of frequencies the response will cover before the NFC falls below 0.3. The NFC of a Dirac delta function is unity throughout the entire frequency domain, with a zero phase shift.

In the frequency domain, the system is represented by its magnitude ratio (MR) and its phase angle (ϕ). These quantities are defined as [4,5,11]:

$$MR = |G(i\omega)| = \sqrt{Re^2(\omega) + Im^2(\omega)} \quad (4)$$

$$\phi = \phi|_{G(\omega)} = \tan^{-1}\left[\frac{\mathrm{Im}(\omega)}{\mathrm{Re}(\omega)}\right] \quad (5)$$

After substitution of the Euler relationship

$$e^{-j\omega x} = \cos(\omega t) - j\sin(\omega t) \quad (6)$$

the real and imaginary contributions can be determined:

$$Re(\omega) = (AC + BD)/(C^2 + D^2) \quad (7a)$$

$$Im(\omega) = (AD - BC)/(C^2 + D^2) \quad (7b)$$

and the values A, B, C, and D are defined as:

$$A = \int_0^{T_y} y(t)\cos(\omega t)\,dt \quad (8a)$$

$$B = \int_0^{T_y} y(t)\sin(\omega t)\,dt \quad (8b)$$

$$C = \int_0^{T_x} x(t)\cos(\omega t)\,dt \quad (8c)$$

$$D = \int_0^{T_x} x(t)\sin(\omega t)\,dt \quad (8d)$$

The computation of these product integrals is carried out numerically using a Filon's Method Data Reduction Code [13]. Application of various quadrature methods such as the trapezoidal rule, Simpson's rule, approximation by linear or higher order curves followed by integration of the subsequent trigonometric functions are discussed in the literature [4,5]. Problems arise due to oscillations of the trigonometric functions at high frequencies. To offer a smooth approximation of the pulse curves, Filon [12] proposed a quadrature formula for the integrals based on approximation by parabolic segments as in Simpson's rule. However, Simpson's rule coefficients are replaced by functions of $\omega\Delta t$ [4]. The transformed, reduced data are plotted as magnitude ratio (MR) and phase angle (ϕ) versus frequency (ω), known as Bode diagrams. These Bode diagrams are analyzed using process control theory to yield transfer functions that empirically model the system.

The MR is the ratio of output to input peak amplitude for a specific frequency when using a direct sinusoidal forcing function. Input and output amplitudes may be measured directly from the time domain data. For pulse testing, the MR must be numerically calculated. For convenience, the input pulse has been approximated as the Dirac delta function.

When taking data from the strip chart recorder, the delay between the input pulse and the output response is typically defined as the pure transport delay, or time delay (θ_d) of the system. As read off the chromatogram, however, this value appears to have an analogous delay contribution. Influences such as pore diffusion and ionic sorption will probably contribute to increase the apparent time delay value. The actual time delay must be calculated from the flow-rate, intraparticular void fraction, column width and length, and column volume, or from a pulse test using a non-interacting protein or chemical. A calculated pure transport delay of approximately 600 s suggests that the strip chart recorder's total delay time of 900 s contains this analogous contribution. By reducing only the response data, the analogous delay contribution becomes apparent at high frequencies on the phase angle Bode plot. Therefore, the time delay analogue is back calculated from the Bode plots. To empirically fit transfer functions to systems with a non-integer order and an analogous time delay, the following equations were proposed:

$$\theta_a = \phi(\omega_i) + \sum_{k=1}^{int(n)} \tan^{-1}(\tau_k\omega_i) + (n - int[n])\tan^{-1}(\tau_n\omega_i) \quad (9)$$

where the subscripts i and k denote the value of the frequency or phase angle at specific points on the Bode diagram, a subscript n denotes a variable's value at the overall system order, t is the time constant ($1/\omega$) at each break point, $\phi(\omega_i)$ is the phase angle at a specified frequency, and θ_a is the time delay analogue. The overall transfer function of the system is calculated using:

$$G(s) = \frac{K_p \exp(-\theta_a s)}{\left(\prod_{k=1}^{int(n)} (\tau_k s + 1)\right)(\tau_n s + 1)^{(n - int(n))}} \quad (10)$$

where s is the Laplace variable and K_p is the steady-state gain of the system. The contributions of each integer order to the overall transfer function are multiplicative in the frequency domain.

3. Procedures

3.1. Materials

Equipment

The equipment consisted of a peristaltic pump (Pharmacia P-1, Piscataway, NJ, USA), 280 nm UV-detector (Pharmacia UV-1), fraction collector (Pharmacia FRAC-100), chart recorder (Pharmacia REC 102), Econo-columns of 10 cm height and 1.0 cm I.D. (Bio Rad, Melville, NY, USA), and silicon tubing (1.0 mm I.D.). The columns were placed with the filter at the same height as the fraction collector's tubing exit, negating any pressure heads. A 50-μl pipetter (Eppendorf North America) was used to insert the pulse into the column.

Chemicals

The wash buffer is 0.1 *M* phosphate buffer, at 7.5 pH. The elution buffer is 1.0 *M* NaCl + 0.1 *M* phosphate buffer, at 7.5 pH. The protein used to pulse the system is 1.0 mg/ml bovine serum albumin (BSA). All chemicals were purchased from Sigma (St. Louis, MO, USA) and meet ACS reagent standards.

Gels

Anion-exchange gels used were DEAE Sephadex, Q-Sepharose, Dowex (200–400 μm), and Dowex (50–100 μm). The gels were all purchased from Sigma.

3.2. Experimental protocol

Gel preparation

The dry gel is allowed to swell overnight in wash buffer. It is then packed into a column and allowed to settle by gravity to a specified height. Once the gel is settled, the column is equilibrated again with wash buffer and the packing height is visually verified. The column is equilibrated with elution buffer and re-equilibrated with wash buffer to remove contaminants and prepare for experimentation.

Experimental

The signal measured is 280 nm UV adsorbance and is directly related to protein concentration at the outlet of the column. Base-line deviations for wash and elution buffers were averaged and accounted for as a 'corrected' base line on the chromatogram. Deviations within 5% of the corrected base line are assumed to be at equilibrium conditions. The flow-rate from the peristaltic pump is held constant at 30 ml/h, except where otherwise noted. Once a column is equilibrated with wash buffer, the flow from the peristaltic pump is stopped, and the column is allowed to drain by gravity until the liquid level is 0.5 cm above the top of the anion-exchange gel packing. At this point the pulse, 50 μl of 1.0 mg/ml BSA, is injected into the top of the column. At the upper surface of the anion-exchange gel, where a thin layer will best simulate the Dirac delta function, the protein is allowed to adsorb via ion-exchange for 2 min. Washing with two column volumes of wash buffer verifies that the protein is bound to the anion-exchange matrix. Next, the protein is isocratically eluted with the elution buffer, and the experiment is concluded when equilibration with elution buffer is complete. All experiments were performed at room temperature (25°C).

Special conditions

DEAE Sephadex was observed to contract in the elution buffer. Although once re-equilibrated with the wash buffer, the gel would expand to its original packed height. Therefore, all packing heights referred to will be pre-elution. The pulsating mechanism of the peristaltic pump is assumed not to be a factor in the pulse tests, as the pulse is one of protein concentration, and not pressure.

3.3. Transfer function

Concentration versus time data (from the chromatogram) is transferred from the UV signal recorder output to a Filon's method data reduction program [13]. The resulting output from this program, in the frequency domain, is used to construct Bode plots. At frequencies high enough to generate oscillatory behavior ($\omega >$ 0.01 Hz), the results were discarded. These oscillations are attributed to the rule-of-thumb: when the normalized frequency content drops below its accepted minimum (NFC < 0.3), the reduced results become scattered [5].

The transfer function is constructed from the Bode plots (Figs. 1a, 1b) as follows: (1) the overall system order is determined from the final slope of the magnitude ratio (MR), (2) the break points are calculated from the intersection of the each asymptote for every integer step in the overall order and the final order, (3) the steady-state gain (K_p) is ascertained from the horizontal asymptote of the MR graph, (4) the time delay analogue (θ_a) is calculated from Eq. 9, and the overall transfer function is calculated using Eq. 10.

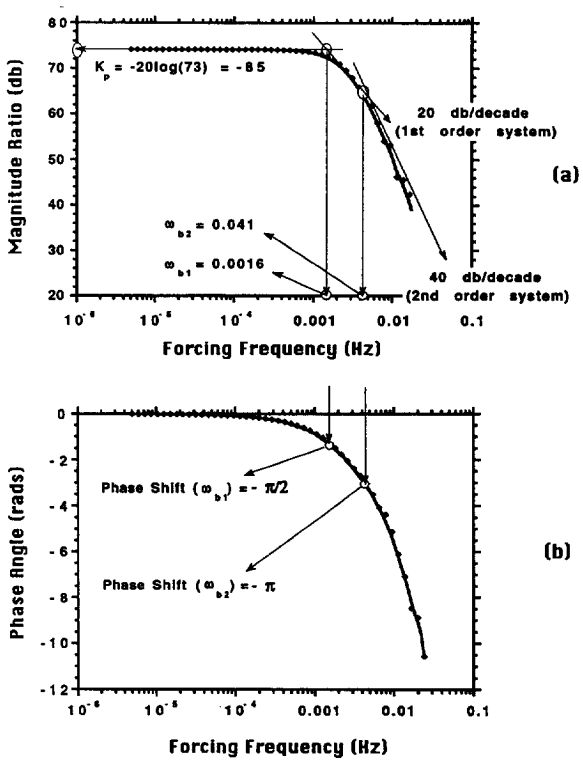

Fig. 1. (a) The magnitude ratio versus forcing frequency Bode plot of an experiment, displaying the log measurement of the breakpoints (ω_{b1} and ω_{b2}), system order (n) and steady-state gain (K_p). (b) The phase angle versus forcing frequency Bode plot of the same experiment, displaying the phase shift at the break points from (a).

4. Results

Transfer functions acquired from the tested systems enable us to empirically model the Bode plots. An example is a transfer function obtained from a 3-cm Sephadex column:

$$G(s) = \frac{-85\exp(-347s)}{(0.0016s+1)(0.041s+1)} \quad (11)$$

It was possible to reproduce the plots from the transfer functions alone (Figs. 2a, 2b) with minimal deviance on either magnitude ratio or phase angle plots versus forcing frequency.

The order of the system (n) was shown to be dependent on the type of anion-exchange gel (Table 1). When each gel was subjected to different packing heights and pulse sample sizes, the order remained constant (Table 1). The system order was reproducible for each experiment with nearly zero deviation for each gel type. A notable exception is that the order of DEAE Sephadex decreased with use as shown in Table 2. It is known that DEAE Sephadex loses activity with use, therefore it is hypothesized that the decrease with system order corresponds to a decrease in the activity of the gel.

The transport delay, timed from pulse elution to initial chromatogram response was equal to the time delay analogue (θ_a) calculated from the Bode plots (Eq. 9). The time delay analogue was reproducible ($\pm 5\%$), and has a linear relationship to the gel packing height of the column (not shown).

As the pulse strength increased, the steady-state gain of the system (K_p) increased as well (Table 1). Although this direct dependence was qualitatively consistent within our experiments, the steady-state gain varied up to 100% of the mean value for each experiment. While the

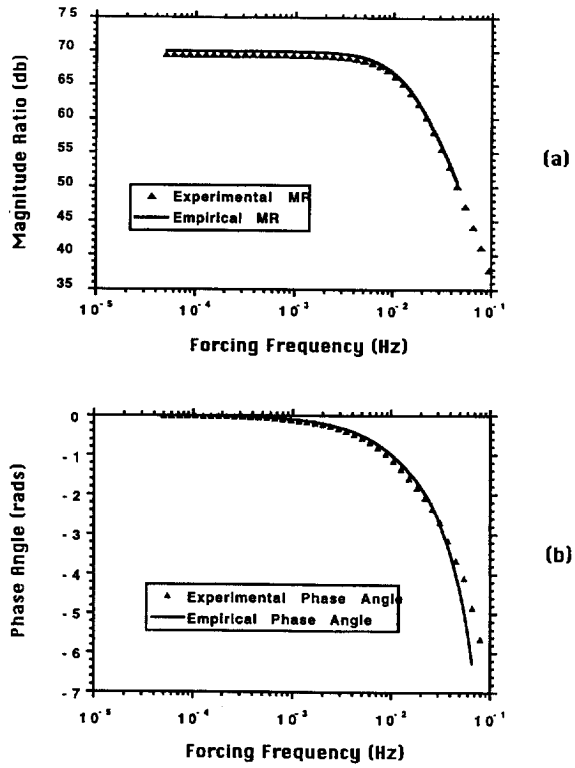

Fig. 2. (a) A comparison of the experimental magnitude ratio (MR) results with the empirical transfer function. (b) For the same experiment, a comparison of the experimental phase angle (ϕ) results with the empirical transfer function.

output of the system is quantifiable by the chromatogram, the input does not have a distinct measurement. The input pulse is assumed to be constant for all experiments (a Dirac delta function), but other contributing factors could lead to the discrepancies. When a method to quantify the input pulse is attained, the steady-state gain of the system should become more stable.

Table 2
The system order versus the age of the anion-exchange gel DEAE Sephadex

Packing height (cm)	System order	
	Initial two days	After four days
3	2	1.25
4	2	1.25
5	2	1.5

5. Conclusion

As a result of this preliminary study, transfer functions have been found to successfully identify properties of a chromatographic system where they have been empirically determined via Bode plots of pulse test experiments. Within the range of values tested, overall system order is dependent on the anion-exchange gel characteristics. In the frequency domain, there is a linear relationship between the time delay analogue of the system and the packing height of the column. This result would suggest that the time delay analogue represents the delay contributions of system characteristics, possibly from diffusion, dispersion, and kinetics. Tests on rate-limited systems would be enlightening in this area.

Table 1
The observed characteristics of anion-exchange gels investigated, including the steady-state gain (K_p), first break point (FBP), and the system order

Gel	Pulse 1[a]			Pulse 2[a]		
	K_p	FBP	Order	K_p	FBP	Order
Dowex (50–100)	7.93	227.36	1.50	20.0	398.0	1.50
Dowex (200–400)	3.16	159.15	1.50	25.0	227.4	1.50
Q-Sepharose	1.78	26.52	2.0	10.0	89.0	2.0
Sephadex (DEAE)	2.51	106.10	2.0	6.33	256.6	2.0

[a] Pulses 1 and 2 were performed with 0.15 mg and 0.32 mg of bovine serum albumin (BSA), respectively.